NRC Research Press

ARTICLE

How distribution characteristics of a soil property affect probabilistic foundation settlement — from the aspect of the first four statistical moments

Yongxin Wu, Yufeng Gao, Limin Zhang, and Jun Yang

Abstract: The effects of the first four statistical moments defining the statistical characteristic of elastic modulus on the probabilistic foundation settlement are investigated in this study. By combining the Hermite probability model and spectral representation method, a method to simulate nonGaussian homogenous fields based on the first four statistical moments is proposed. Linear elastic finite element models are employed to study the total settlement and the differential settlement of a shallow foundation. Probabilistic measurements of total–differential settlement obtained by the Monte Carlo simulations are presented. For the cases considered, the effects of skewness and kurtosis defining the probabilistic characteristic of elastic modulus on the total–differential settlement of a probabilistic foundation are illustrated. The computed results show that the value of skewness has a more significant effect on the probabilistic foundation settlement than kurtosis, and the case with the smallest skewness is observed as the most critical one.

Key words: random field, spectral representation method, soil variability, foundation settlement, differential settlement, Monte Carlo.

Résumé : Les effets des quatre premiers moments statistiques définissant la caractéristique statistique du module d'élasticité sur le tassement probabiliste des fondations sont étudiés dans cette étude. En combinant le modèle de probabilité de Hermite et la méthode de représentation spectrale, une méthode de simulation du champ homogène non gaussien basée sur les quatre premiers moments statistiques est proposée. Des modèles élastiques linéaires par éléments finis sont utilisés pour étudier le tassement total et le tassement différentiel d'une fondation peu profonde. Les mesures probabilistes du tassement total–différentiel obtenues par les simulations de Monte Carlo sont présentées. Pour les cas considérés, les effets de l'asymétrie et de l'aplatissement définissant la caractéristique probabiliste du module d'élasticité sur le tassement total-différentiel d'une fondation probabiliste sont illustrés. Les résultats calculés montrent que la valeur de l'asymétrie a un effet plus important sur le tassement probabiliste des fondations que l'aplatissement, et le cas de la plus petite asymétrie est considéré comme le plus critique. [Traduit par la Rédaction]

Mots-clés : champ aléatoire, méthode de représentation spectrale, variabilité du sol, tassement des fondations, tassement différentiel, Monte Carlo.

1. Introduction

Soil properties always exhibit considerable spatial variation because soils are always formed in different physical and chemical conditions. This spatial variation brings uncertainties in the estimation of soil parameters. The uncertainties arise from several sources such as inherent soil variability, measurement errors, and model transformation uncertainties (Phoon and Kulhawy 1999). Furthermore, when the failure mode of the involved geotechnical problem is considered, additional uncertainties hidden in quantities in the calculation models exist (Rackwitz 2000). The theory of random fields is traditionally applied to define the spatial variability of soil properties by introducing correlation models.

In the last decade, with the aid of high-speed computers, the effects of stochastic soil properties on various problems in geomechanics were assessed. For instance, a series of studies investigated the effects of spatial variability of soil properties on settlements of foundations (Fenton and Griffiths 2002, 2005; Liu et al. 2015), on the bearing capacity of shallow foundations (Griffiths and Fenton 2001; Griffiths et al. 2002; Fenton and Griffiths 2003; Popescu et al. 2005*a*; Cho and Park 2010; Li et al. 2015; Wu et al. 2019), on the stability of slopes (Sivakumar Babu and Mukesh 2004; Griffiths and Fenton 2004; Griffiths et al. 2009; Srivastava and Babu 2009; Cho 2010; Zhang et al. 2013, 2018; Li et al. 2014, 2016, 2018; Jiang et al. 2015; Zhu et al. 2017; Ji et al. 2019), on soil liquefaction (Popescu et al. 1997, 2005*b*), and on the seismic site response (Rathje et al. 2010; Bradley 2013; Johari and Momeni 2015). These studies illustrate the importance of considering the spatial variability of soil properties in geotechnical design. In particular, by considering the spatial variability of soil properties, the reliability of geotechnical designs is increased. Furthermore, failure modes, such as nonsymmetric failure modes and differential settlements, which cannot be observed under the assumption of homogeneous soil, can be identified by considering the spatial variability of soil properties.

Received 12 February 2019. Accepted 28 March 2019.

Y. Wu and Y. Gao. Key Laboratory of Ministry of Education for Geomechanics and Embankment Engineering, Hohai University, No. 1, Xikang Road, Nanjing, 210098, China.
L. Zhang. Department of Civil and Environmental Engineering, The Hong Kong University of Science and Technology, Clear Water Bay, Hong Kong.
J. Yang. Department of Civil Engineering, The University of Hong Kong, Pokfulam Road, Hong Kong.
Corresponding author: Yufeng Gao (email: yfgao66@163.com).

Copyright remains with the author(s) or their institution(s). Permission for reuse (free in most cases) can be obtained from RightsLink.

The settlement of foundations is a classical geotechnical subject with considerable interest, and the effects of spatial variability of soil properties on settlements also attracted wide attention as aforementioned. The problems of total–differential settlements of shallow foundations on spatially varying soil have been investigated by many methods, such as analytical method (Frantziskonis and Breysse 2003), the stochastic finite element method (Baecher and Ingra 1981; Brząkała and Puła 1996), the stochastic integral formulation method (Zeitoun and Baker 1992), and the Monte Carlo simulation (MCS). Among these methods, the MCS is one of the most widely used. To study the settlement of shallow foundations, several authors have discussed the effect of variability of elastic modulus on the settlement results by considering the influence of the mean value, the standard deviation, and scale of fluctuation. While two-dimensional (2D) models have been applied in most cases, Fenton and Griffiths (2005) studied the probability distribution of total settlement and differential settlements by using a fully three-dimensional (3D) model.

When investigating the effects of spatial variability of soil properties on settlements, it is generally assumed (but not always) that the parameter of elastic modulus follows the lognormal distribution, which is mathematically convenient and can avoid producing negative values of soil properties. However, based on several studies reported in the literature, soil properties can follow different probability distributions for different types of soils and sites (Wang et al. 2015). Furthermore, Popescu et al. (2005*a*) demonstrated that the distribution type of the soil shear strength has a considerable influence on the bearing capacity of foundations. Similarly, Zhou et al. (1999) showed that the distribution type of the coefficient of radial consolidation has a significant impact on the consolidation results. In addition, Jimenez and Sitar (2009) investigated the effects of the distribution type characterizing the spatial variability of Young's modulus on the settlement of shallow foundation, and found that the distribution type of elastic modulus have a significant impact on the computed settlement results. In all, the distribution type of soil properties should be considered when conducting the reliability analysis for geotechnical design. However, how the distribution characteristic affects the probabilistic settlement has never been studied.

In practical applications, the probabilistic density function (PDF), or equivalently the cumulative distribution function (CDF), of soil properties may be difficult to obtain. Recently, Bayesian methods have been developed to address this issue by integrating limited measurement data with prior knowledge (Wang and Cao 2013; Wang et al. 2016; Cao et al. 2016). Generally, the probabilistic characteristic of soil properties can be easily expressed by the statistical moments, which can be obtained from the measured data (Zhao and Lu 2006). In this study, the effects of the first four statistical moments to define the probabilistic characteristic of soil properties on the total–differential settlements of shallow foundations are investigated, and the way how the third moment and fourth moment work on the probabilistic settlements is illustrated.

The remaining portion of this paper is organized as follows. In the following section, the method to simulate nonGaussian homogenous fields based on the first four statistical moments is proposed by combining the Hermite probability model (HPM) and spectral representation method (SRM). Then, the finite element models employed to investigate the total settlement and the differential settlement of a shallow foundation are presented. In the finite element models, the random fields of elastic modulus are simulated by the proposed method. Finally, the results of foundation settlements computed by the MCSs are discussed, and the effects of skewness and kurtosis defining the probabilistic characteristic of elastic modulus on probabilistic foundation settlements are illustrated.

2. Simulation of nonGaussian homogeneous fields based on first four statistical moments

Several methods such as the midpoint method (Der Kiureghian and Ke 1988), the local average subdivision (LAS) method (Fenton and Vanmarcke 1990), the shape function method (Liu et al. 1986), turning bands methods (TBM) (Matheron 1973), the Karhunen–Loève (KL) expansion (Phoon et al. 2002), the SRM (Popescu et al. 1998), and the linear estimation method (Liu et al. 2014) can be used to discretize the random field. Fenton (1994) systematically investigated the characteristics of three common random field generators (i.e., SRM, TBM, and LAS), and gave a number of useful and helpful guidelines and suggestions to choose the algorithm in the application. In this study, the SRM, which has been proved to provide a better accuracy in terms of autocorrelation function and lower order moments (Stefanou and Papadrakakis 2007), is employed.

The SRM is one of the most widely used methods in the simulation of random processes as well as random fields. Given that this part mainly focuses on simulation of random fields, the following representative papers related to simulating random fields based on the SRM are mentioned here. The SRM was established by Yaglom (1962) and Shinozuka and Jan (1972) for the simulation of one-dimensional (1-D), univariate formulation and extended by Shinozuka and Deodatis (1996) to simulate multi-dimensional Gaussian random fields. With regard to simulating nonGaussian random fields, Yamazaki and Shinozuka (1988) firstly proposed an iterative method based on the SRM to simulate 1-D nonGaussian random fields by the translation process theory. Popescu et al. (1998) extended Yamazaki and Shinozuka's method to simulate multi-variate, multi-dimensional, nonGaussian random fields. Recently, Wu et al. (2017) proposed a simple and efficient iterative scheme to simulate multi-variate, multi-dimensional, non-Gaussian random fields based on the SRM. In this paper, the basic idea of the simple and efficient iterative scheme is used and combined with the theory of HPM to simulate random fields defined by the given autocorrelation function and the first four statistical moments. For simplicity, the method to simulate a 2D homogeneous nonGaussian random field will be described herein. In fact, the following method can easily be extended to the 3D case.

Consider a 2D homogeneous nonGaussian random field $y(x, z)$, which is completely defined by autocorrelation function $\rho_{NG}(\xi_x, \xi_z)$, where ξ_x and ξ_y are the distance in horizontal and vertical directions, respectively, and the first statistical moments (i.e., mean value μ_f, standard deviation σ_f, skewness, and kurtosis). Without loss of generality, $y(x, z)$ can be standardized to $\bar{y}(x, z) = [y(x, z) - \mu_f]/\sigma_f$, which is with zero mean value and unit variance.

2.1. Hermite probability model (HPM) based on first four statistical moments

The Hermite polynomial function is an adequate model to translate the underlying standard Gaussian field $\bar{g}(x, z)$ to the target standard nonGaussian field $\bar{y}(x, z)$ (Grigoriu 1984). For a 2D random field, the transformation based on the Hermite polynomial is

$$\bar{y}(x, z) = k\{\bar{g}(x, z) + c[\bar{g}(x, z)^2 - 1] + d[\bar{g}(x, z)^3 - 3\bar{g}(x, z)]\} \quad (1)$$

where

$$k = \frac{1}{\sqrt{1 + 2c^2 + 6d^2}} \quad (2)$$

In eq. (1), k is a scaling factor that ensures unit variance of $\bar{y}(x, z)$. The coefficients c and d can be determined by the prescribed skewness (Sk) and kurtosis (Ku) according to the following relationships (Gurley et al. 1997):

$$\text{Sk} = k^3(8c^3 + 108cd^2 + 36cd + 6c) \tag{3}$$

$$\text{Ku} = k^4(60c^4 + 3348d^4 + 2232c^2d^2 + 60c^2 + 252d^2 + 1296d^3 + 576c^2d + 24d + 3) \tag{4}$$

To obtain the values of c and d in eq. (1), the set of nonlinear equations aforeshown can be solved through numerical iteration or closed form approximate solution given by Yang et al. (2013). When the translation parameters c and d are determined, the PDF of the target standard nonGaussian field $\bar{f}(x, z)$ is given by (Yang and Gurley 2015)

$$f_y(y) = \frac{1}{\sqrt{2\pi}} \exp\left[-\frac{u^2(y)}{2}\right]\frac{du(y)}{dy} \tag{5}$$

where

$$u(y) = [\sqrt{\xi^2(y) + r} + \xi(y)]^{1/3} - [\sqrt{\xi^2(y) + r} - \xi(y)]^{1/3} - a \tag{6}$$

$$\xi(y) = 1.5\frac{1}{3d}\left(\frac{c}{3d} + \frac{y}{k}\right) - \left(\frac{c}{3d}\right)^3 \tag{7}$$

$$r = \left[\frac{1}{3d} - \left(\frac{c}{3d}\right)^2 - 1\right]^3 \tag{8}$$

and u and r are two intermediate variables as utilized in the right part of eqs. (5) and (6), respectively.

The HPM is very robust over a wide range of values for skewness and kurtosis, exhibiting even strongly nonGaussian behavior (Yang et al. 2013). It was found that many PDFs (e.g., lognormal distribution) can be approximated by the HPM probability models according to the corresponding skewness and kurtosis. It means that, the HPM can be considered as a potential probability model for any process–field with skewness and kurtosis values within the admissible range.

2.2. Simulation of 2D homogeneous Gaussian fields

For a 2D homogenous Gaussian field $g(x, z)$, its correlation structure can be defined by its autocorrelation function $\rho_G(\xi_x, \xi_z)$. By using the 2D version of the Wiener–Khintchine transform, the target Gaussian power spectral density (PSD) function can be obtained

$$S_G(\kappa_x, \kappa_z) = \frac{1}{(2\pi)^2}\int_{-\infty}^{+\infty}\int_{-\infty}^{+\infty}\rho_G(\xi_x, \xi_z)e^{-i(\kappa_x\xi_x + \kappa_z\xi_z)}\,d\xi_x\,d\xi_z \tag{9}$$

where ξ_x and ξ_z are the distance in horizontal and vertical directions, respectively; and κ_x and κ_z are the wave numbers in horizontal and vertical directions, respectively.

For random fields of soil properties, the PSD function at eq. (9) is symmetric with respect to the origin

$$S_G(\kappa_x, \kappa_z) = S_G(\kappa_x, -\kappa_z) = S_G(-\kappa_x, \kappa_z) = S_G(-\kappa_x, -\kappa_z) \tag{10}$$

Then, samples of the 2D homogeneous Gaussian field can be simulated by the following series:

$$g(x, z) = \sum_{l_1=0}^{N_1-1}\sum_{l_2=0}^{N_2-1}\sqrt{S_G(\kappa_{xl_1}, \kappa_{zl_2})\Delta\kappa_x\Delta\kappa_z} \times\left[\cos\left(\kappa_{xl_1}x + \kappa_{zl_2}z + \phi^1_{l_1l_2}\right) + \cos\left(\kappa_{xl_1}x - \kappa_{zl_2}z + \phi^2_{l_1l_2}\right)\right] \tag{11}$$

where

$$\kappa_{xl_i} = l_i\Delta\kappa_x \qquad \kappa_{zl_i} = l_i\Delta\kappa_z \qquad l_i = 0, 1, \ldots, N_i - 1 \tag{12}$$

$$\Delta\kappa_x = \kappa_{xu}/N_1 \qquad \Delta\kappa_z = \kappa_{zu}/N_2 \tag{13}$$

and κ_{xu} and κ_{zu} are the upper cut-off wave numbers in the direction x and z, respectively. N_1, N_2 are the number of points used for the discretization of the PSD function along the x and z axes, $\Delta\kappa_x$ and $\Delta\kappa_z$ are the discretization steps in the wave number domain. $\phi^1_{l_1l_2}$ and $\phi^2_{l_1l_2}$ are two sets of N_1N_2 independent random phase angles uniformly distributed over the interval $[0, 2\pi]$.

According to the central limit theorem, the simulated random fields are asymptotically Gaussian as N_1 and N_2 approaching infinity simultaneously. In addition, the fast Fourier transform (FFT) technique can be applied to simulate the random field with high efficiency.

2.3. NonGaussian translation field theory

The basic idea of nonGaussian translation field theory is that a homogeneous nonGaussian field can be obtained through nonlinear transformation of a homogeneous Gaussian field (called "underlying Gaussian field"). The method was introduced by Grigoriu (1984) and has been applied to 1-D fields. In this paper the same approach was applied to a multi-dimensional field.

The Hermite polynomial function is an adequate model to translate the underlying standard Gaussian field $\bar{g}(x, z)$ to the target standard nonGaussian field $\bar{y}(x, z)$. A 2D nonGaussian random field can be mapped from an underlying standard Gaussian field $\bar{g}(x, z)$ based on the transformation shown in eq. (1). As this is a nonlinear transformation, the correlation structure of the random field will be changed. By using the transformation field theory, the relationship between the nonGaussian autocorrelation function $\rho_{NG}(\xi_x, \xi_z)$ and the Gaussian autocorrelation function $\rho_G(\xi_x, \xi_z)$ can be explicitly expressed as (Yang and Gurley 2015)

$$\rho_{NG}(\xi_x, \xi_z) = k^2[\rho_G(\xi_x, \xi_z) + 2c^2\rho^2_G(\xi_x, \xi_z) + 6d^2\rho^3_G(\xi_x, \xi_z)] \tag{14}$$

It has been observed that the autocorrelation and marginal distribution of translation fields cannot be both prescribed arbitrarily, because such pairs may be incompatible. It means that, for an arbitrarily given pair of PSD function (or equivalently autocorrelation function) and nonGaussian PDF (or the first four statistical moments), it is impossible to estimate an exact underlying Gaussian PSD function. Several reasons cause this "incompatibility" as summarized by Shields et al. (2011), Shields and Deodatis (2013), and Wu et al. (2018). However, for practical applications it is usually possible to find a translation field that approximates very well any prescribed incompatible pair. In the following section, the iterative scheme to find the underlying PSD function will be discussed in detail.

2.4. Simulation of 2D homogeneous nonGaussian fields

To simulate a standard homogeneous non-Gaussian random field $\bar{y}(x, z)$, the classic SRM and nonGaussian translation field theory were combined. The flowchart of the method is shown in Fig. 1, and the general steps of the simulation method can be summarized as

1. Estimate an underlying Gaussian PSD function of the standard Gaussian field.
2. Simulate an underlying Gaussian random field using the estimated underlying Gaussian PSD function through the SRM presented in eq. (11).
3. Translate the underlying standard Gaussian random field to a standard nonGaussian random field through eq. (1).

Fig. 1. Flowchart of proposed method to simulate nonGaussian random field. g_{min}, solution for $\bar{y}(x, z) = -1/\mathrm{Cov}_y$ in eq. (1).

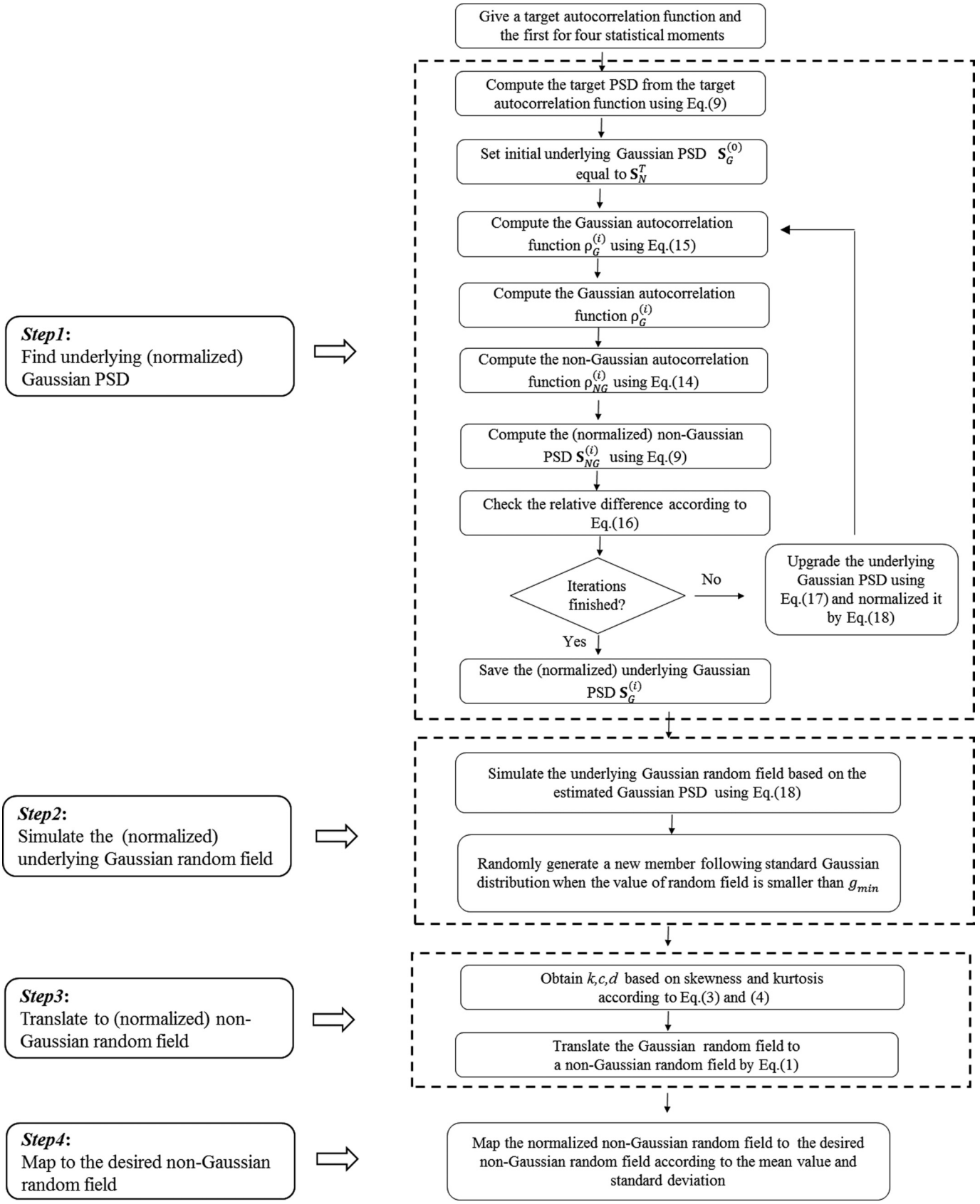

4. Map the standard nonGaussian random field into the desired nonGaussian random field by using $y(x, z) = \bar{y}(x, z)\sigma_f + \mu_f$.

In the aforementioned steps, the key point is to estimate the underlying Gaussian PSD function. Once the underlying Gaussian PSD function is determined, the samples of the target nonGaussian random field can easily be obtained by utilizing the SRM and translation theory. For this purpose, the iterative scheme to find an approximate underlying Gaussian PSD function proposed by Shields et al. (2011) and Shields and Deodatis (2013) can be easily introduced into this method as follows.

The general steps of the proposed iterative scheme for estimating the underlying Gaussian PSD function are described in detail as follows.

1. *Initialize the underlying Gaussian* PSD *function* — In the iterative scheme, the first step is to provide an initial guess for the underlying Gaussian PSD function. To get a high convergence rate, it is recommended to assume that the initial underlying Gaussian PSD function $S_G^{(0)}(\kappa_x, \kappa_z)$ is equal to the target nonGaussian PSD function $S_{NG}^{T}(\kappa_x, \kappa_z)$.
2. *Compute Gaussian autocorrelation function* — At iteration (i), the Gaussian autocorrelation function $\rho_G^{(i)}(\xi_x, \xi_z)$ can be obtained from the Gaussian PSD function $S_G^{(i)}(\kappa_x, \kappa_z)$ through the 2D Winner–Khinchine equation

$$\rho_G^{(i)}(\xi_x, \xi_z) = \int_{-\infty}^{+\infty}\int_{-\infty}^{+\infty} S_G^{(i)}(\kappa_x, \kappa_z) e^{i(\kappa_x\xi_x + \kappa_z\xi_z)}\, d\kappa_x\, d\kappa_z \quad (15)$$

where superscript (i) indicates the ith iteration of the algorithm.
3. *Computer nonGaussian autocorrelation function* — Once the Gaussian autocorrelation function $\rho_G^{(i)}(\xi_x, \xi_z)$ is given, the corresponding nonGaussian autocorrelation function $\rho_{NG}^{(i)}(\xi_x, \xi_z)$ can be obtained through the translation filed theory (shown in eq. (14)).
4. *Compute nonGaussian* PSD *function* — The nonGaussian PSD function $S_{NG}^{(i)}(\kappa_x, \kappa_z)$ is determined from the nonGaussian autocorrelation function $\rho_{NG}^{(i)}(\xi_x, \xi_z)$ by means of the inverse version of 2D Wiener–Khintchine transform (shown in eq. (9)).
5. *Check relative errors of nonGaussian* PSD *function* — At each iteration, to decide whether the iteration will be ended or not, a convergence criterion should be checked. The error measures the discrepancy between the computed nonGaussian PSD function $S_{NG}^{(i)}(\kappa_x, \kappa_z)$ and the target nonGaussian PSD function $S_{NG}^{T}(\kappa_x, \kappa_z)$ is defined as

$$\varepsilon^{(i)} = \frac{\int_{-\infty}^{+\infty}\int_{-\infty}^{+\infty} \left| S_N^{T}(\kappa_x, \kappa_z) - S_N^{(i)}(\kappa_x, \kappa_z) \right| d\kappa_x\, d\kappa_z}{\int_{-\infty}^{+\infty}\int_{-\infty}^{+\infty} S_N^{T}(\kappa_x, \kappa_z)\, d\kappa_x\, d\kappa_z} \quad (16)$$

When the error stabilizes or becomes small enough (e.g., for 2D cases 1% usually yields good accuracy), the current underlying Gaussian PSD function is saved. Otherwise, the upgrading of underlying Gaussian PSD function $S_{NG}^{(i)}(\kappa_x, \kappa_z)$ should be performed.
6. *Upgrade underlying Gaussian* PSD *function* — The underlying Gaussian PSD function $S_{NG}^{(i)}(\kappa_x, \kappa_z)$ is upgraded by

$$S_G^{(i+1)}(\kappa_x, \kappa_z) = \left[\frac{S_N^{T}(\kappa_x, \kappa_z)}{S_N^{(i)}(\kappa_x, \kappa_z)}\right]^{\beta} S_G^{(i)}(\kappa_x, \kappa_z) \quad (17)$$

where β is selected to optimize the convergence rate. After upgrading, the new Gaussian PSD function $S_{NG}^{(i+1)}(\kappa_x, \kappa_z)$ is obtained, and it is positive definite. However, the variance of the underlying Gaussian PSD function may be changed. Thus, the estimated Gaussian PSD function $S_{NG}^{(i+1)}(\kappa_x, \kappa_z)$ should be normalized by

$$S_G^{N(i+1)}(\kappa_x, \kappa_z) = \frac{S_G^{(i+1)}(\kappa_x, \kappa_z)}{\int_{-\infty}^{+\infty}\int_{-\infty}^{+\infty} S_G^{(i+1)}(\kappa_x, \kappa_z)\, d\kappa_x\, d\kappa_z} \quad (18)$$

where the superscript "N" denotes the normalization.

Fig. 2. Geometry of model: (*a*) single footing; (*b*) two footings.

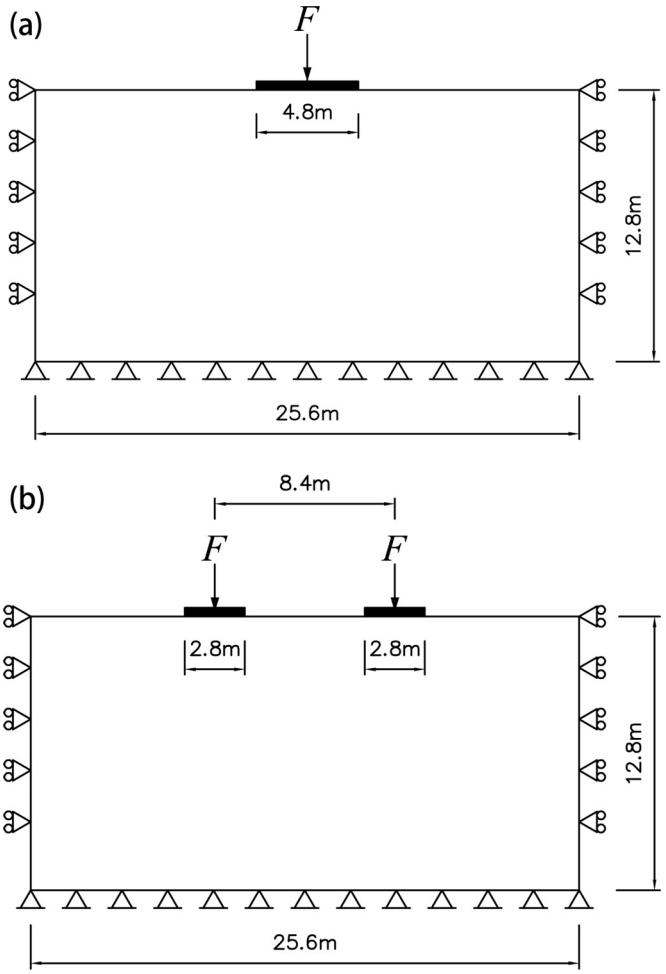

2.5. Avoiding negative values

For many random fields defining soil properties (e.g., elastic modulus and untrained shear strength), the value of these random fields should be positive. However, as the target PDF is defined by eq. (5), which allows the appearance of values from negative infinite to positive infinite theoretically, the method proposed abovecannot ensure all the samples of the simulated fields take on a positive value. To ensure the positive value of the simulated sample fields, the following scheme is proposed.

For a random field $y(x, z)$ with a coefficient of variation (Cov) $\mathrm{Cov}_y = \sigma_y/\mu_y$, to make sure all sample fields have positive values, the minimum value of the standard field $\bar{y}(x, z)$ (standardized by $\bar{y}(x, z) = [y(x, z) - \mu_y]/\sigma_y$) should be larger than $-1/\mathrm{Cov}_y$. According to the relationship shown in eq. (1), the minimum value of the standard field $\bar{g}(x, z)$ should be larger than g_{min}, which is the solution for $\bar{y}(x, z) = -1/\mathrm{Cov}_y$ in eq. (1). It means that, the generation of positive samples will, in turn, require the preliminary generation

Fig. 3. Target PDFs of elastic modulus: (*a*) Sk = 0; (*b*) Sk = 0.5; (*c*) Sk = 1.0; (*d*) Sk = 1.5.

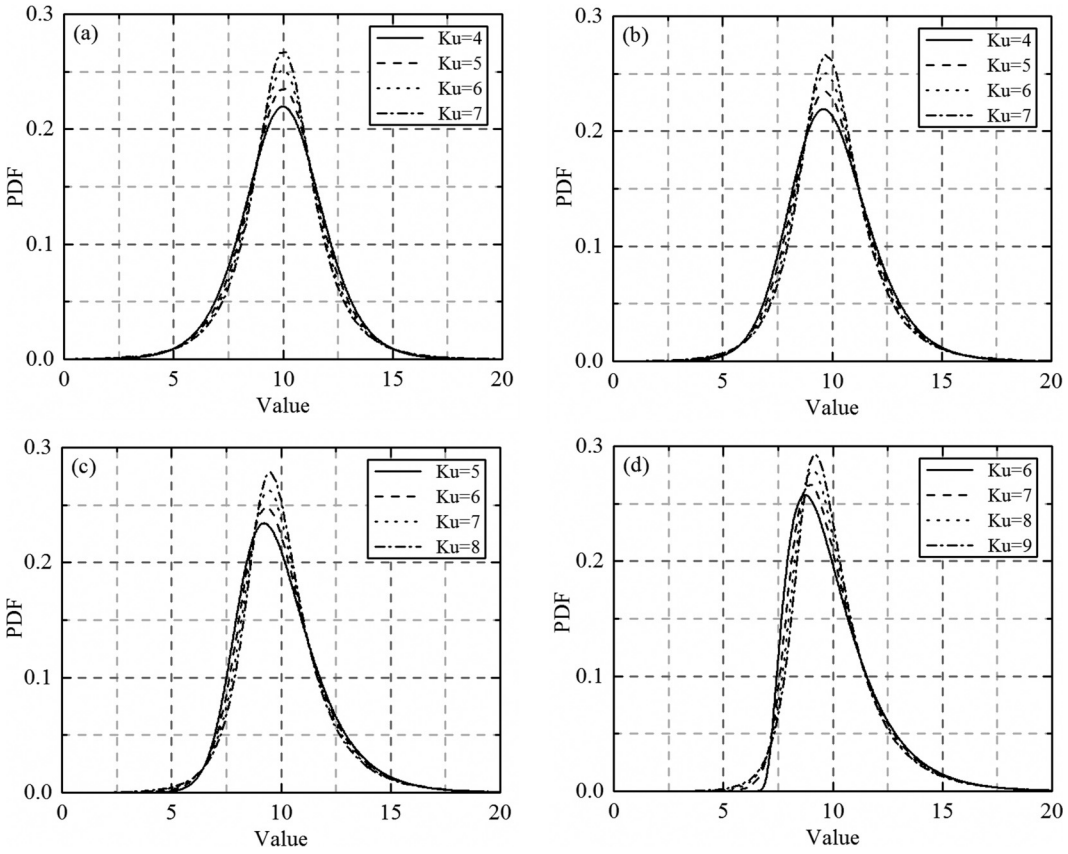

of standard Gaussian samples whose minimum value is larger than g_{min}. To generate such a standard Gaussian sample, the basic idea of generation truncated Gaussian samples can be applied. The ideal is that, when the value of the sample is smaller than g_{min}, one must randomly generate a new number that follows standard Gaussian distribution and is larger than g_{min}. Then the positive value of samples of the described random fields can be guaranteed. In fact, for small value of g_{min}, this scheme has little influence on the prescribed characteristic (e.g., autocorrelation function, and the first four statistical moments) of the target random field.

3. Finite element model

Now, probabilistic measures of total settlement and differential settlement are presented. Because settlements are usually computed using elasticity theory in typical foundation design, two 2D linear elastic finite element models are employed to investigate the total settlement and the differential settlement of a shallow foundation with spatially random soil, respectively. The first model is shown in Fig. 2*a*, in which a single footing is applied to a soil layer to estimate the basic probabilistic behavior of total settlement. In the second model, shown in Fig. 2*b*, the issue of differential settlements under a pair of footings is addressed. In both models, the sizes of soil mass are the same, with 25.6 m in the horizontal direction and 12.8 m in the vertical direction. To use the FFT technique in the MCSs, the soil mass is discretized into 128 four noded quadrilateral elements in the horizontal direction by 64 elements in the vertical direction. For the single footing case, the footing width is 4.8 m, and for the two footings case, the width of footings is 2.8 m, and the distance between footings centers is 8.4 m. The design load(s) F applied on the top of the footing(s) are set to be 300 kN.

In both cases, the footing(s) are considered to be rigid and have a rough interface with the underlying soil. Rotations of foundation(s) are not allowed, and it is assumed that there is no slipping between the foundation and the underlying soil. Horizontal movement is restrained on the side boundaries where only vertical movement is allowed, while both horizontal and vertical movements are restrained on the bottom of the soil body.

Because of elastic finite element models are used, only elastic modulus and Poisson ratio should be given. A constant Poisson ratio fixed at 0.25 is used in this study given that Poisson ratio has a secondary influence on the results of settlement (Fenton and Griffiths 2002). Elastic modulus E is considered to be spatially random. The simulation method proposed in this study is applied to generate the samples of random fields of elastic modulus E. A squared exponential 2D autocorrelation function is applied to define the spatial correlation of elastic modulus as follows (Jiang et al. 2014):

$$\rho(\xi_x, \xi_z) = \exp\left\{-\left[(\xi_x/l_x)^2 + (\xi_z/l_z)^2\right]\right\} \quad (19)$$

where l_x and l_z are the autocorrelation distances defining the decay rates in the horizontal and vertical directions, respectively. In this study, the assumption of isotropy is adopted, and the autocorrelation distances in both directions are set to be 10 m.

To investigate the effect of skewness and kurtosis on probabilistic measures of settlements, the mean value of elastic modulus E is set to be 10 MPa, and standard deviation of elastic modulus E is fixed at 2 MPa, which means the value of Cov is 0.2. Although, it may be more reasonable to model the mean value of elastic modulus with an increasing linear trend (Li et al. 2014), the random field of elastic modulus is assumed to be stationary as done by

Fig. 4. Comparison lognormal distribution with HPM probabilistic model: (*a*) in linear scale; (*b*) in semi-log scale.

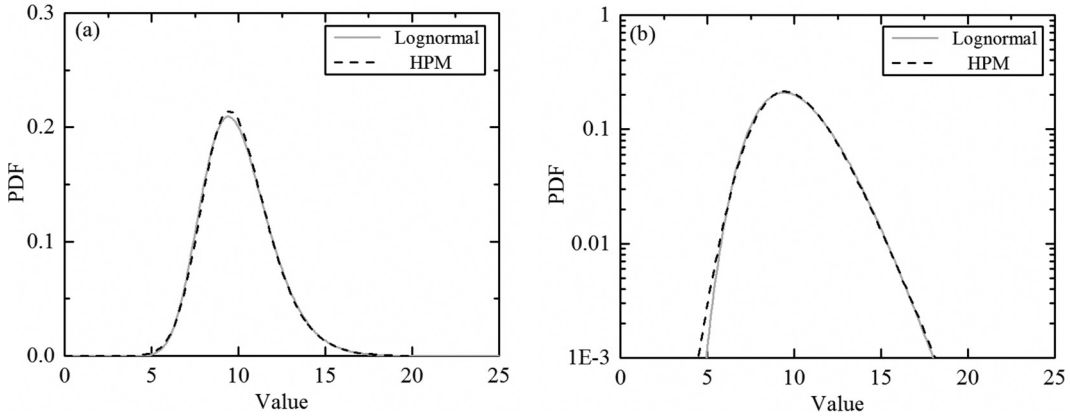

Fenton and Griffiths (2002, 2005). The involved target PDFs defined by the HPM according to the value of skewness and kurtosis are shown in Fig. 3. It is observed that the PDFs of the HPM cover a wide range of scales by changing the values of Sk and Ku. It should be mentioned that only nonnegative values of skewness are considered because the PDFs of soil properties are usually positively skewed or symmetrical (Popescu et al. 2005).

At this juncture, the capacity of the HPM to approximate the lognormal distribution is demonstrated. The skewness and kurtosis corresponding to the prescribed lognormal distribution are 0.608 and 3.664, respectively. The lognormal distribution and HPM probabilistic model according to the corresponding skewness and kurtosis are plotted in linear scale and in semi-log scale (as shown in Fig. 4), respectively. It is observed that the HPM closely approximates the lognormal PDF. Furthermore, a similarly good match can be found in many (but not all) other applications of PDFs. This demonstrates that the proposed method based on the HPM is worthy of consideration even when the user wishes to impart a specific target PDF rather than just the first four statistical moments.

Based on coordinates of elements in the finite element models, a series of realizations of random fields are generated to provide values of elastic modulus by the proposed method. A typical realization of random field is shown in Fig. 5. Some typical PDFs of the simulated random field are plotted in Fig. 6, and compared with the target one. The PDFs are estimated by the "ksdensity()" function in Matlab. The result shows that they match the target ones very well.

The output variable of the model is the vertical displacement of the central point of the footing(s), and downward movement is considered to be positive.

4. Computed results

We perform extensive MCSs using the finite element model presented in section 3. The extensive Monte Carlo analysis involves simulation of a set of random fields for elastic modulus E, which is followed by a batch program conducting a set of conventional deterministic settlement analyses using ABAQUS. Finally, the settlement of footing(s) for each realization is retrieved.

4.1. Single footing case

In the single footing case, 1000 simulations were considered enough to give reasonably stable and reproducible statistical output. Figure 7 shows the mean value and standard deviation of the total settlement δ as a function of the number of simulations N_{sim} for a typical example. It is observed that stable results can be obtained as N_{sim} reaches 1000. Furthermore, the PDF of the total settlement δ is also considered (as shown in Fig. 8). Given that the PDF of N_{sim} = 1000 is very close to that of N_{sim} = 2000. 1000 realizations were considered to be economic in time without loss of accuracy. It is noted that attention is not paid to the very small probability level in this paper. If the very small probability level is investigated, the number of MCS samples required shall depend on the probability level targeted.

Fig. 5. Typical realization of random field of elastic modulus. [Color online.]

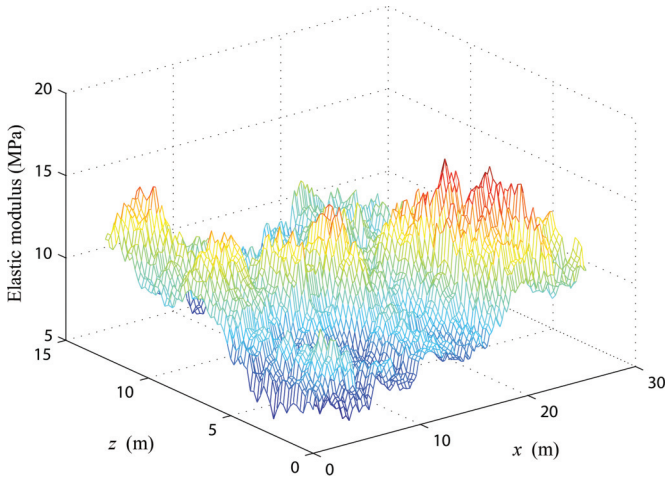

Following a suit of MCSs, the mean and standard deviation of the total settlement δ for different combinations of Sk and Ku can be determined, and have been shown in Table 1 and Table 2, respectively. It can be found that the distribution characteristic has little effect on the mean value of the total settlement, but greatly affects the standard deviation of the total settlement. From the aspect of high statistical moments, the parameter of skewness has a significant effect on the standard deviation of the total settlement. In general, with the increase of skewness, the standard deviation of the total settlement decreases. Taking the case of Ku = 6 for example, the standard deviation of the total settlement deceases by 21.9% from 4.399 mm (for Sk = 0) to 3.435 mm (for Sk = 1.5). Furthermore, the mean value of the total settlement can be predicted by

$$E(\delta) = \exp\left[\ln(\delta_{det}) + \sigma_E^2/2\right] \quad (20)$$

where δ_{det} is the "deterministic" settlement obtained from the finte element method analysis when the modulus of all elements are set to be μ_E, which is 10 MPa in this study. The value of δ_{det} for the example investigated is 34.24 mm, then, according to

Fig. 6. Comparing PDFs of simulated sample of random field with target: (*a*) Sk = 0.5, Ku = 5; (*b*) Sk = 1.5, Ku = 6.

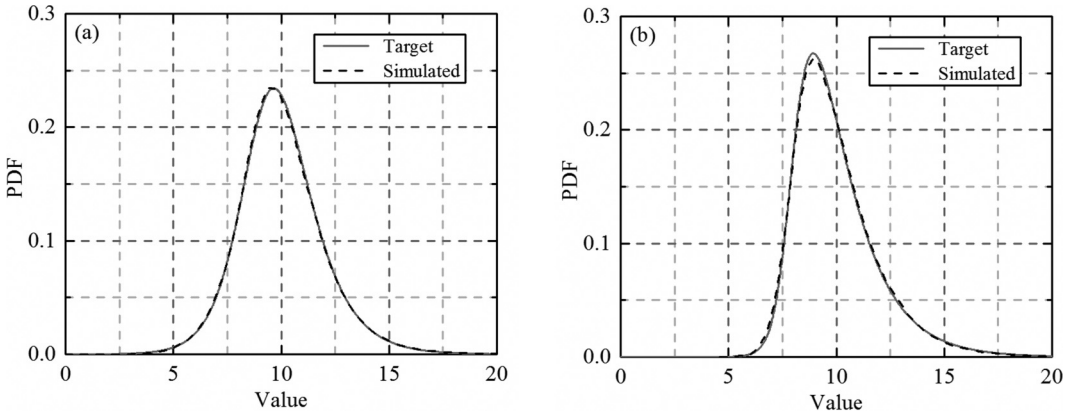

Fig. 7. Mean value and standard deviation of total settlement as function of number of simulations: (*a*) mean value; (*b*) standard deviation.

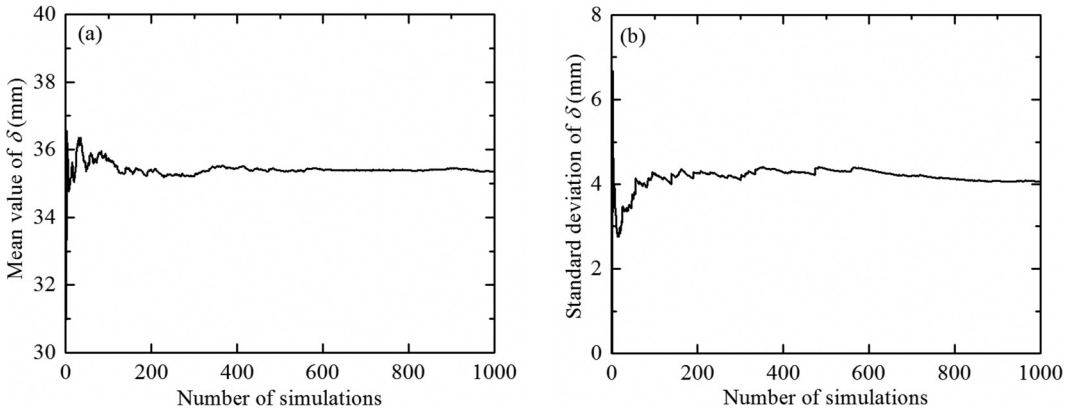

Fig. 8. PDFs of total settlement for different number of simulations.

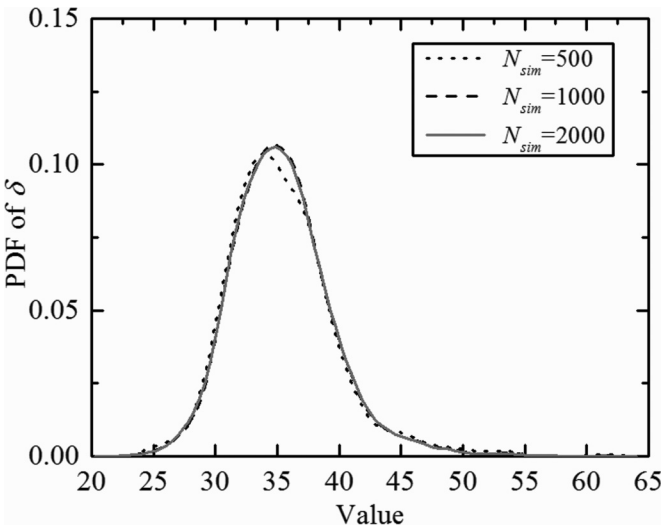

Table 1. Mean value of total settlement.

	Mean value of total settlement (mm)					
Sk	Ku = 4	Ku = 5	Ku = 6	Ku = 7	Ku = 8	Ku = 9
0	35.37	35.34	35.41	35.47	—	—
0.5	35.14	35.12	35.14	35.14	—	—
1.0	—	35.24	35.20	35.21	35.27	—
1.5	—	—	35.14	35.10	35.23	35.11

Table 2. Standard deviation of total settlement.

	Standard deviation of total settlement (mm)					
Sk	Ku = 4	Ku = 5	Ku = 6	Ku = 7	Ku = 8	Ku = 9
0	4.43	4.67	4.40	4.48	—	—
0.5	3.84	3.91	4.06	3.98	—	—
1.0	—	3.68	3.53	3.67	3.94	—
1.5	—	—	3.44	3.39	3.31	3.43

eq. (20), $E(\delta)$ should be 34.92 mm. The estimated mean value of total settlement for all the cases is very close to the predicated value.

Fenton and Griffiths (2002) pointed out that the total settlement can be presented well by a lognormal distribution if the elastic modulus E is also lognormally distributed. From the knowledge of basic statistics, if the input elastic modulus does not follow a lognormal distribution, the distribution of output settlement may be changed. To show how the input distribution affects the distribution of output settlement, the PDFs of the estimated PDFs of the total settlement were investigated, and comparisons were conducted with the lognormal distribution corresponding to the estimated mean value and standard deviation (Fig. 9). In the case of Sk = 0.5, a good match between the estimated PDF of total settlement and the corresponding lognormal PDF is observed, because the value of skewness is very close to the skewness of lognormal distribution (i.e., 0.608). While, in the cases of symmetrical distribution (Sk = 0) and highly skewed distribution (i.e., Sk = 1.5) of the elastic modulus, the lognormal distribution of total settlement cannot be accepted because the estimated PDF differs from the corresponding lognormal PDF. It means that, if SK of

Fig. 9. Comparison of estimated PDFs of total settlement with corresponding lognormal distributions: (*a*) Sk = 0; (*b*) Sk = 0.5; (*c*) Sk = 1.0; (*d*) Sk = 1.5.

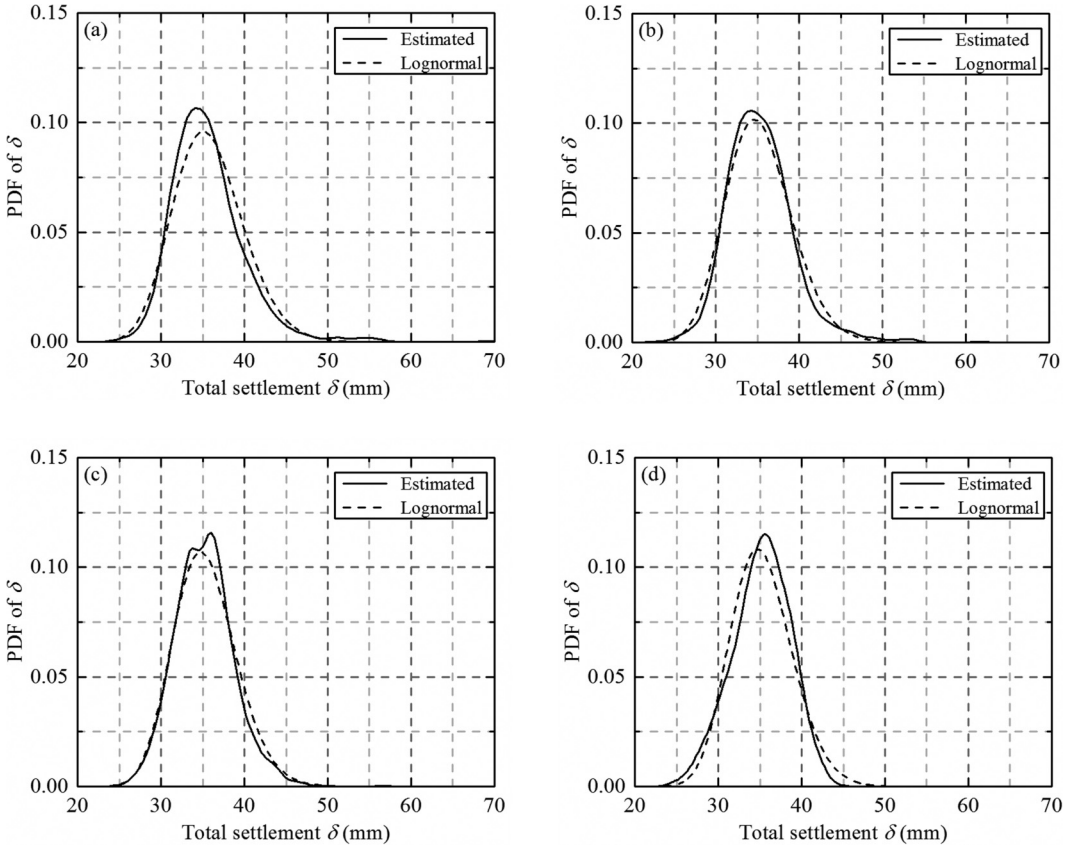

Table 3. Probability of total settlement exceeding a certain value.

		Probability of total settlement exceeding a certain value (%)								
Sk	Ku	$\alpha = 1$	$\alpha = 1.1$	$\alpha = 1.2$	$\alpha = 1.3$	$\alpha = 1.4$	$\alpha = 1.5$	$\alpha = 1.6$	$\alpha = 1.7$	$\alpha = 1.8$
0	4	53.8	24.1	9.2	3.1	1.3	0.6	0.4	0.3	0.2
	5	53.4	22.8	8.6	4.0	2.3	1.6	0.7	0.4	0
	6	58.9	24.7	9.3	3.3	1.5	1.1	0.5	0.1	0
	7	56.9	22.8	9.5	3.6	1.9	0.9	0.4	0.3	0.2
0.5	4	57.0	23.8	6.2	1.6	0.5	0.1	0	0	0
	5	57.1	23.9	6.9	1.7	0.5	0.2	0	0	0
	6	58.5	23.4	6.7	2.7	1.2	0.6	0.1	0	0
	7	54.4	21.6	8.2	2.7	1.1	0.2	0.1	0	0
1.0	5	59.2	24.6	6.9	0.8	0.1	0	0	0	0
	6	59.1	21.5	5.0	0.9	0.2	0.1	0	0	0
	7	59.9	22.7	5.8	1.3	0.3	0.2	0	0	0
	8	58.8	22.2	7.4	2.4	1.3	0.5	0.1	0	0
1.5	6	62.4	24.1	2.9	0.1	0	0	0	0	0
	7	60.8	21.4	4.0	0.6	0	0	0	0	0
	8	64.0	21.0	4.2	0.5	0.1	0	0	0	0
	9	61.6	21.9	4.6	0.4	0	0	0	0	0

elastic modulus is close to the skewness of lognormal distribution (i.e., 0.608), the assumption that the total settlement follows lognormal distribution (as proposed by Fenton and Griffiths 2002) is also acceptable.

In practice, the estimated displacement under expected service load should not be greater than a selected limiting tolerable displacement. Therefore, the probability that the value of total displacement exceeds some thresholds is investigated. Table 3 shows the probability, $P(\delta > \alpha\delta_{det})$, for α varying from 1 to 1.8, where α is the constant selected to control the threshold. It is found that, for the case of $\alpha = 1$, with the increasing of skewness, the probability of the total settlement exceeding the "deterministic" settlement increases. However, for the case of high value of α, with the increasing of skewness, the probability of the total settlement exceeding the value, $\alpha\delta_{det}$, decreases. It means the extremely high values of total settlement usually occur in low skewed cases. These extremely high values of total settlement can be explained by the heavy tails with small value of the elastic modulus. Meanwhile, the CDFs of the computed total settlements are plotted in Fig. 10. It is also found that, for smaller skewness of elastic modulus, the CDFs of estimated total settlement have longer tails. In all, the case with smaller skewness of elastic modulus can be considered as the worse one because it exhibits more probabilities in high values of total settlement.

Fig. 10. Estimated cumulative distribution functions (CDFs) of total settlement: (*a*) Ku = 6; (*b*) Sk = 1.0.

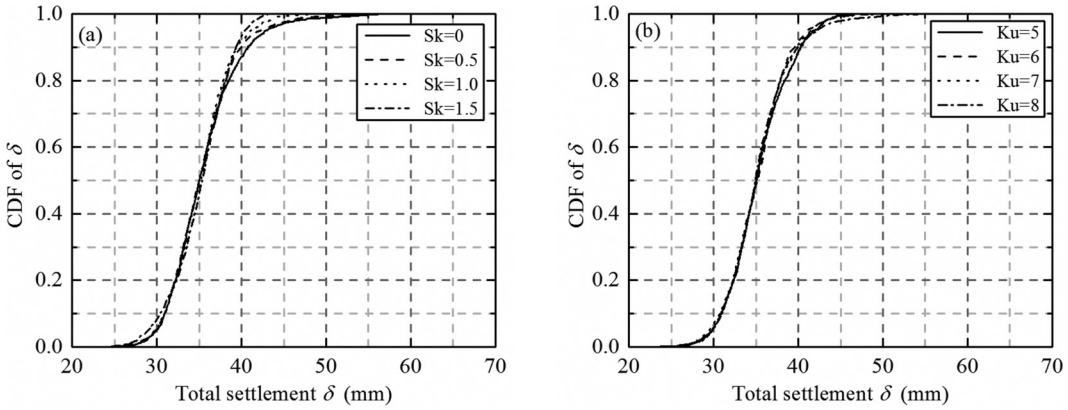

Fig. 11. Mean value and standard deviation of differential settlement as function of number of simulations: (*a*) mean value; (*b*) standard deviation.

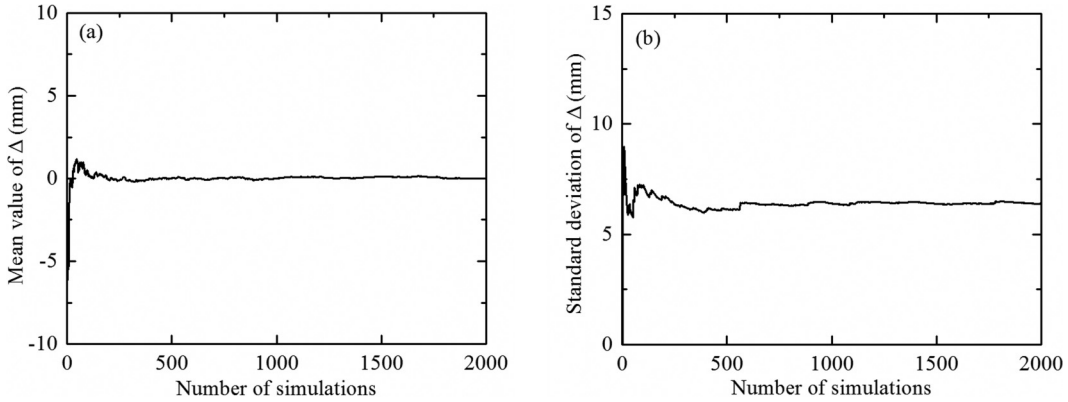

Fig. 12. PDFs of differential settlement for different number of simulations.

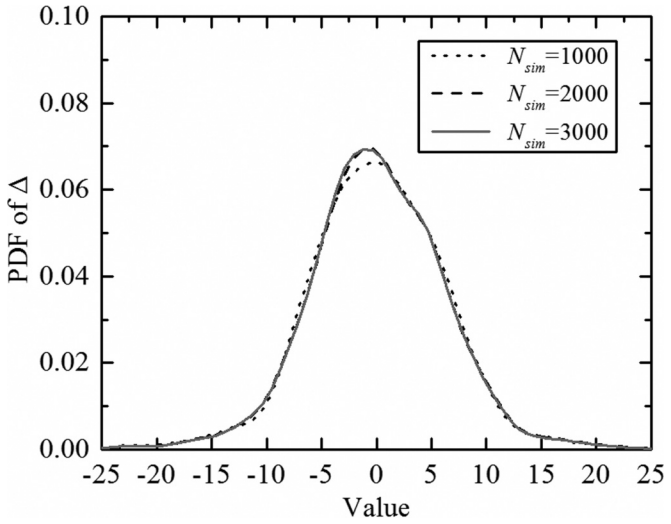

Table 4. Mean value of absolute differential settlement.

	Mean value of absolute differential settlement (mm)					
Sk	Ku = 4	Ku = 5	Ku = 6	Ku = 7	Ku = 8	Ku = 9
0	4.97	4.78	4.96	4.97	—	—
0.5	4.64	4.74	4.78	4.79	—	—
1.0	—	4.37	4.51	4.61	4.33	—
1.5	—	—	4.11	4.14	4.04	4.08

Table 5. Standard deviation of absolute differential settlement.

	Standard deviation of absolute differential settlement (mm)					
Sk	Ku = 4	Ku = 5	Ku = 6	Ku = 7	Ku = 8	Ku = 9
0	4.32	4.98	5.22	5.00	—	—
0.5	3.75	4.11	4.26	4.23	—	—
1.0	—	3.32	3.67	3.82	3.68	—
1.5	—	—	3.07	3.09	3.00	3.16

Table 6. Probability of absolute differential settlement exceeding a certain value.

		Probability of absolute differential settlement exceeding a certain value (%)					
Sk	Ku	$\beta = 1$	$\beta = 1.2$	$\beta = 1.4$	$\beta = 1.6$	$\beta = 1.8$	$\beta = 2$
0	4	0.7	1.3	2.1	3.9	5.1	7.4
	5	0.9	1.9	3.0	4.4	6.0	7.4
	6	1.9	2.7	3.5	4.7	5.8	8.3
	7	1.0	2.5	3.9	5.4	6.6	8.6
0.5	4	0.2	0.6	1.0	1.9	3.4	5.3
	5	0.5	0.8	1.8	2.4	3.9	6.2
	6	0.4	1.1	1.8	3.3	4.5	5.6
	7	0.4	0.9	2.4	3.0	4.7	6.3
1.0	5	0	0	0.3	1.0	2.0	3.7
	6	0.1	0.6	0.8	1.4	2.5	4.5
	7	0.2	0.4	0.8	2.3	3.7	5.2
	8	0.4	0.7	0.9	1.5	2.8	4.0
1.5	6	0	0.1	0.2	0.4	0.8	2.0
	7	0	0	0.2	0.4	1.1	2.7
	8	0	0	0.2	0.5	0.9	2.0
	9	0	0.1	0.3	0.5	1.6	2.4

Fig. 13. Estimated CDFs of absolute differential settlement: (*a*) Ku = 6; (*b*) Sk = 1.0.

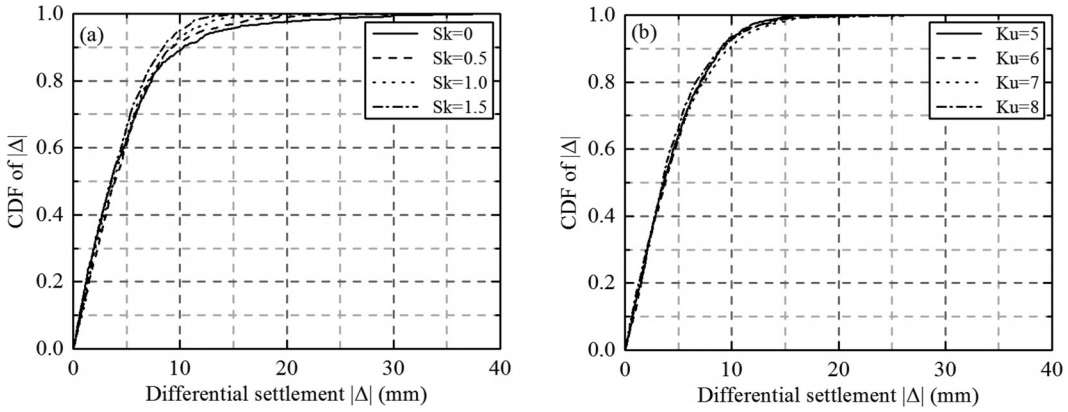

4.2. Two footing case

Consider now the case of two footings shown in Fig. 1*b*. Assume that the settlements, δ_1 and δ_2, are the settlement of the left footing and that of the right footing, respectively. The differential settlement is defined as

$$\Delta = \delta_1 - \delta_2 \quad (21)$$

In the two footing case, 2000 simulations were considered enough to give stable outputs. Figure 11 shows the mean value and standard deviation of the differential settlement Δ as a function of the number of simulations N_{sim} for a typical example. Figure 12 shows the PDFs of the differential settlement for different number of simulations. From the results shown in Figs. 11 and 12, N_{sim} = 2000 is acceptable.

In practice, more attention should be paid to the absolute value of differential settlement. Attention can now be turned to the absolute value of differential settlement. Following a suit of MCSs, the mean and standard deviation of the absolute differential settlement, |Δ|, for different combinations of skewness and kurtosis can be determined, and have been shown in Tables 4 and 5, respectively. It is found that both the mean value and standard deviation of the absolute differential settlement are affected by the distribution characteristic (Fig. 13). Compared to kurtosis, skewness has a more significant effect. Generally, with the increase of skewness, both the mean value and standard deviation of the absolute differential settlement decrease. Taking the cases of Ku = 6 for example, the mean value deceases by 16.9% from 4.956 (for Sk = 0) to 4.111 (for Sk = 1.5), and the standard deviation deceases by 41.2% from 5.222 (for Sk = 0) to 3.069 (for Sk = 1.5).

To avoid upper-structure damage, the absolute differential settlement should be limited to a certain value, e.g., $|\Delta|_{lim} = D/360$ (Fenton and Griffiths 2002), which is 23.3 mm in this study, where D is the distance between footings centers. The probability that the value of the absolute differential settlement exceeds some threshold is investigated. Table 3 shows the probability, $P(|\Delta| > |\Delta|_{lim}/\beta)$ (with β varying from 1 to 2), representing the probability of differential settlement exceeding the limit value $|\Delta|_{lim}$ when the load is β times of the design load F (i.e., F = 300 KN). It is found that, with the increasing of skewness, the probability of the absolute differential settlement exceeding $|\Delta|_{lim}/\beta$ increases. It means that the extremely high values of absolute differential settlement usually occur in low skewed cases of elastic modulus. Meanwhile, the CDFs of the computed differential settlements are plotted in Fig. 12. It is also found that, for smaller value of skewness, the CDFs of estimated total settlement have longer tails. In all, the case of smaller value of skewness can be considered as worse because it produces more probabilities in high values of differential settlement.

5. Conclusions

The effects of the first four statistical moments defining the statistical characteristic of elastic modulus on the probabilistic foundation settlement were investigated. To that end, a method to simulate nonGaussian homogenous field based on the first four statistical moments was proposed. This method combines the theory of HPM and SRM, and it provides a way to generate random field of soil properties, whose distribution characteristic is defined by the first four statistical moments. The proposed method was utilized to simulate the random field of elastic modulus for the study of probabilistic characteristic of the total settlement and the differential settlement of shallow foundations. On the basis of the Monte Carlo simulations (MCSs), the following observations can be made:

1. Skewness and kurtosis of elastic modulus have little effect on the mean value of the total settlement, but they, especially the value of skewness, greatly affect the standard deviation of the total settlement. Compared to kurtosis, skewness of elastic modulus has a more significant effect on the distribution characteristic of total settlement, and the case with smallest value of skewness is considered as the most dangerous one.
2. Skewness of elastic modulus affects both the mean and standard deviation of the absolute differential settlement, and the influence of skewness is more significant. Similar to the results of total settlement, the skewness of elastic modulus has a more significant effect on the distribution characteristic of differential settlement, and the case with smallest value of skewness is considered as the most dangerous one.

The results of this study suggest that the identification of the skewness of elastic modulus is extremely important. In practice, more attention should be paid to low skewed case because it may result in an unexpected large total settlement or differential settlement. However, the aforementioned results are obtained based on certain autocorrelation structures; the effects of autocorrelation structure on the results are not discussed, which needs to be further investigated.

One of the most important contributions of this study is the concept of estimating the probabilistic characteristic of (differential) settlement of shallow foundations based on the first four moments of elastic modulus. The present study paves the way towards better estimation of probabilistic foundation settlement. However, a simple and general way to calculate the probability of (differential) settlement exceeding a certain value is yet to be found. The proposed method to simulate nonGaussian homogenous field based on the first four statistical moments can be applied to simulate other random fields in civil engineering.

Acknowledgements

Support from the National Natural Science Foundation of China (grant No. 41630638) and the National Key Research and Development Program of China (grant No. 2016YFC0800205) is greatly acknowledged.

References

Baecher, G.B., and Ingra, T.S. 1981. Stochastic FEM in settlement predictions. Journal of the Geotechnical Engineering Division, ASCE, **107**(4): 449–463.

Bradley, B.A. 2013. A critical examination of seismic response uncertainty analysis in earthquake engineering. Earthquake Engineering & Structural Dynamics, **42**(11): 1717–1729. doi:10.1002/eqe.2331.

Brząkała, W., and Puła, W. 1996. A probabilistic analysis of foundation settlements. Computers and Geotechnics, **18**(4): 291–309. doi:10.1016/0266-352X(95)00033-7.

Cao, Z., Wang, Y., and Li, D. 2016. Quantification of prior knowledge in geotechnical site characterization. Engineering Geology, **203**: 107–116. doi:10.1016/j.enggeo.2015.08.018.

Cho, S.E. 2010. Probabilistic assessment of slope stability that considers the spatial variability of soil properties. Journal of Geotechnical and Geoenvironmental Engineering, **136**(7): 975–984. doi:10.1061/(ASCE)GT.1943-5606.0000309.

Cho, S.E., and Park, H.C. 2010. Effect of spatial variability of cross-correlated soil properties on bearing capacity of strip footing. International Journal of Numerical and Analytical Methods in Geomechanics, **34**(1): 1–26.

Der Kiureghian, A., and Ke, J.-B. 1988. The stochastic finite element method in structural reliability. Probabilistic Engineering Mechanics, **3**(2): 83–91. doi:10.1016/0266-8920(88)90019-7.

Fenton, G.A. 1994. Error evaluation of three random-field generators. Journal of Engineering Mechanics, **120**(12): 2478–2497. doi:10.1061/(ASCE)0733-9399(1994)120:12(2478).

Fenton, G.A., and Griffiths, D.V. 2002. Probabilistic foundation settlement on spatially random soil. Journal of Geotechnical and Geoenvironmental Engineering, **128**(5): 381–390. doi:10.1061/(ASCE)1090-0241(2002)128:5(381).

Fenton, G.A., and Griffiths, D.V. 2003. Bearing-capacity prediction of spatially random c-ϕ soils. Canadian Geotechnical Journal, **40**(1): 54–65. doi:10.1139/t02-086.

Fenton, G.A., and Griffiths, D.V. 2005. Three-dimensional probabilistic foundation settlement. Journal of Geotechnical and Geoenvironmental Engineering, **131**(2): 232–239. doi:10.1061/(ASCE)1090-0241(2005)131:2(232).

Fenton, G.A., and Vanmarcke, E.H. 1990. Simulation of random fields via local average subdivision. Journal of Geotechnical and Geoenvironmental Engineering, **116**(8): 232–239. doi:10.1061/(ASCE)0733-9399(1990)116:8(1733).

Frantziskonis, G., and Breysse, D. 2003. Influence of soil variability on differential settlements of structures. Computers and Geotechnics, **30**(3): 217–230. doi:10.1016/S0266-352X(02)00062-9.

Griffiths, D.V., and Fenton, G.A. 2001. Bearing capacity of spatially random soil: the undrained clay Prandtl problem revisited. Géotechnique, **51**(4): 351–359. doi:10.1680/geot.2001.51.4.351.

Griffiths, D.V., and Fenton, G.A. 2004. Probabilistic slope stability analysis by finite elements. Journal of Geotechnical and Geoenvironmental Engineering, **130**(5): 507–518. doi:10.1061/(ASCE)1090-0241(2004)130:5(507).

Griffiths, D.V., Fenton, G.A., and Manoharan, N. 2002. Bearing capacity of rough rigid strip footing on cohesive soil: probabilistic study. Journal of Geotechnical and Geoenvironmental Engineering, **128**(9): 743–755. doi:10.1061/(ASCE)1090-0241(2002)128:9(743).

Griffiths, D.V., Huang, J., and Fenton, G.A. 2009. Influence of spatial variability on slope reliability using 2-D random fields. Journal of Geotechnical and Geoenvironmental Engineering, **135**(10): 1367–1378. doi:10.1061/(ASCE)GT.1943-5606.0000099.

Grigoriu, M. 1984. Crossings of non-Gaussian translation process. Journal of Engineering Mechanics, **110**(4): 610–620. doi:10.1061/(ASCE)0733-9399(1984)110:4(610).

Gurley, K.R., Tognarelli, M.A., and Kareem, A. 1997. Analysis and simulation tools for wind engineering. Probabilistic Engineering Mechanics, **12**(1): 9–31. doi:10.1016/S0266-8920(96)00010-0.

Ji, J., Zhang, C., Gao, Y., and Kodikara, J. 2018. Effect of 2D spatial variability on slope reliability: a simplified FORM analysis. Geoscience Frontiers, **9**(6): 1631–1638. doi:10.1016/j.gsf.2017.08.004.

Ji, J., Zhang, C., Gao, Y., and Kodikara, J. 2019. Reliability-based design for geotechnical engineering: an inverse FORM approach for practice. Computers and Geotechnics, **111**: 22–29. doi:10.1016/j.compgeo.2019.02.027.

Jiang, S., Li, D., Zhang, L., and Zhou, C. 2014. Slope reliability analysis considering spatially variable shear strength parameters using a non-intrusive stochastic finite element method. Engineering Geology, **168**: 120–128. doi:10.1016/j.enggeo.2013.11.006.

Jiang, S., Li, D., Cao, Z., Zhou, C., and Phoon, K.K. 2015. Efficient system reliability analysis of slope stability in spatially variable soils using Monte Carlo simulation. Journal of Geotechnical and Geoenvironmental Engineering, **141**(2): 04014096. doi:10.1061/(ASCE)GT.1943-5606.0001227.

Jimenez, R., and Sitar, N. 2009. The importance of distribution types on finite element analyses of foundation settlement. Computers and Geotechnics, **36**(3): 474–483. doi:10.1016/j.compgeo.2008.05.003.

Johari, A., and Momeni, M. 2015. Stochastic analysis of ground response using non-recursive algorithm. Soil Dynamics and Earthquake Engineering, **69**: 57–82. doi:10.1016/j.soildyn.2014.10.025.

Li, D., Qi, X., Phoon, K.-K., Zhang, L., and Zhou, C. 2014. Effect of spatially variable shear strength parameters with linearly increasing mean trend on reliability of infinite slopes. Structural Safety, **49**: 45–55. doi:10.1016/j.strusafe.2013.08.005.

Li, D., Xiao, T., Cao, Z., Zhou, C., and Zhang, L. 2016. Enhancement of random finite element method in reliability analysis and risk assessment of soil slopes using Subset Simulation. Landslides, **13**(2): 293–303. doi:10.1007/s10346-015-0569-2.

Li, J., Tian, Y., and Cassidy, M.J. 2015. Failure mechanism and bearing capacity of footings buried at various depths in spatially random soil. Journal of Geotechnical and Geoenvironmental Engineering, **141**(2): 04014099. doi:10.1061/(ASCE)GT.1943-5606.0001219.

Liu, W.K., Belytschko, T., and Mani, A. 1986. Random field finite elements. International Journal for Numerical Methods in Engineering, **23**(10): 1831–1845. doi:10.1002/nme.1620231004.

Liu, Y., Lee, F.-H., Quek, S.T., and Beer, M. 2014. Modified linear estimation method for generating multi-dimensional multi-variate Gaussian field in modelling material properties. Probabilistic Engineering Mechanics, **38**: 42–53. doi:10.1016/j.probengmech.2014.09.001.

Liu, Y., Lee, F.H., Quek, S.T., Chen, E.J., and Yi, J.T. 2015. Effect of spatial variation of strength and modulus on the lateral compression response of cement-admixed clay slab. Géotechnique, **65**(10): 851–865. doi:10.1680/jgeot.14.P.254.

Matheron, G. 1973. The intrinsic random functions and their applications. Advances in Applied Probability, **5**: 439–468. doi:10.2307/1425829.

Phoon, K.-K., and Kulhawy, F.H. 1999. Characterization of geotechnical variability. Canadian Geotechnical Journal, **36**(4): 612–624. doi:10.1139/t99-038.

Phoon, K.K., Huang, S.P., and Quek, S.T. 2002. Implementation of Karhunen-Loeve expansion for simulation using a wavelet-Galerkin scheme. Probabilistic Engineering Mechanics, **17**(3): 293–303. doi:10.1016/S0266-8920(02)00013-9.

Popescu, R., Prevost, J.H., and Deodatis, G. 1997. Effects of spatial variability on soil liquefaction: some design recommendations. Géotechnique, **47**(5): 1019–1036. doi:10.1680/geot.1997.47.5.1019.

Popescu, R., Deodatis, G., and Prevost, J.H. 1998. Simulation of homogeneous non-Gaussian stochastic vector fields. Probabilistic Engineering Mechanics, **13**(1): 1–13. doi:10.1016/S0266-8920(97)00001-5.

Popescu, R., Deodatis, G., and Nobahar, A. 2005*a*. Effects of random heterogeneity of soil properties on bearing capacity. Probabilistic Engineering Mechanics, **20**(4): 324–341. doi:10.1016/j.probengmech.2005.06.003.

Popescu, R., Prevost, J.H., and Deodatis, G. 2005*b*. 3D effects in seismic liquefaction of stochastically variable soil deposits. Géotechnique, **55**(1): 21–31. doi:10.1680/geot.2005.55.1.21.

Rackwitz, R. 2000. Reviewing probabilistic soils modelling. Computers and Geotechnics, **26**(3–4): 199–223. doi:10.1016/S0266-352X(99)00039-7.

Rathje, E.M., Kottke, A.R., and Trent, W.L. 2010. Influence of input motion and site property variabilities on seismic site response analysis. Journal of Geotechnical and Geoenvironmental Engineering, **136**(4): 607–619. doi:10.1061/(ASCE)GT.1943-5606.0000255.

Shields, M.D., and Deodatis, G. 2013. A simple and efficient methodology to approximate a general non-Gaussian stationary stochastic vector process by a translation process with applications in wind velocity simulation. Probabilistic Engineering Mechanics, **31**: 19–29. doi:10.1016/j.probengmech.2012.10.003.

Shields, M.D., Deodatis, G., and Bocchini, P. 2011. A simple and efficient methodology to approximate a general non-Gaussian stationary stochastic process by a translation process. Probabilistic Engineering Mechanics, **26**(4): 511–519. doi:10.1016/j.probengmech.2011.04.003.

Shinozuka, M., and Deodatis, G. 1996. Simulation of multi-dimensional Gaussian stochastic fields by spectral representation. Applied Mechanics Reviews, **49**(1): 29–53. doi:10.1115/1.3101883.

Shinozuka, M., and Jan, C.-M. 1972. Digital simulation of random processes and its applications. Journal of Sound and Vibration, **25**(1): 111–128. doi:10.1016/0022-460X(72)90600-1.

Sivakumar Babu, G.L., and Mukesh, M.D. 2004. Effect of soil variability on reliability of soil slopes. Géotechnique, **54**(5): 335–337. doi:10.1680/geot.2004.54.5.335.

Srivastava, A., and Babu, G.L.S. 2009. Effect of soil variability on the bearing capacity of clay and in slop stability problems. Engineering Geology, **108**(1–2): 142–152. doi:10.1016/j.enggeo.2009.06.023.

Stefanou, G., and Papadrakakis, M. 2007. Assessment of spectral representation and Karhunen-Loève expansion methods for the simulation of Gaussian stochastic fields. Computer Methods in Applied Mechanics and Engineering, **196**(21–24): 2465–2477. doi:10.1016/j.cma.2007.01.009.

Wang, Y., and Cao, Z.J. 2013. Probabilistic characterization of Young's modulus of soil using equivalent samples. Engineering Geology, **159**: 106–118. doi:10.1016/j.enggeo.2013.03.017.

Wang, Y., Zhao, T., and Cao, Z. 2015. Site-specific probability distribution of

geotechnical properties. Computers and Geotechnics, **70**: 159–168. doi:10.1016/j.compgeo.2015.08.002.

Wang, Y., Cao, Z., and Li, D. 2016. Bayesian perspective on geotechnical variability and site characterization. Engineering Geology, **203**: 117–125. doi:10.1016/j.enggeo.2015.08.017.

Wu, Y., Li, R., Gao, Y., Zhang, N., and Zhang, F. 2017. Simple and efficient method to simulate homogenous multidimensional non-Gaussian vector fields by the spectral representation method. Journal of Engineering Mechanics, **143**(12): 06017016. doi:10.1061/(ASCE)EM.1943-7889.0001368.

Wu, Y., Gao, Y., Zhang, N., and Zhang, F. 2018. Simulation of spatially varying non-Gaussian and non-stationary seismic ground motions by the spectral representation method. Journal of Engineering Mechanics, **144**(1): 04017143. doi:10.1061/(ASCE)EM.1943-7889.0001371.

Wu, Y., Zhou, X., Gao, Y., Zhang, L., and Yang, J. 2019. Effect of soil variability on bearing capacity accounting for non-stationary characteristics of undrained shear strength. Computers and Geotechnics, **110**: 199–210. doi:10.1016/j.compgeo.2019.02.003.

Yaglom, A.M. 1962. An introduction to the theory of stationary random functions. Dover, Mineola, N.Y.

Yamazaki, F., and Shinozuka, M. 1988. Digital generation of non-Gaussian stochastic fields. Journal of Engineering Mechanics, **114**(7): 1183–1197. doi:10.1061/(ASCE)0733-9399(1988)114:7(1183).

Yang, L., and Gurley, K.R. 2015. Efficient stationary multivariate non-Gaussian simulation based on a Hermite PDF model. Probabilistic Engineering Mechanics, **42**: 31–41. doi:10.1016/j.probengmech.2015.09.006.

Yang, L., Gurley, K.R., and Prevatt, D.O. 2013. Probabilistic modeling of wind pressure on low-rise buildings. Journal of Wind Engineering and Industrial Aerodynamics, **114**(2): 18–26. doi:10.1016/j.jweia.2012.12.014.

Zeitoun, D.G., and Baker, R. 1992. A stochastic approach for settlement predictions of shallow foundations. Géotechnique, **42**(4): 617–629. doi:10.1680/geot.1992.42.4.617.

Zhang, F., Gao, Y.F., Wu, Y., and Zhang, N. 2018. Upper-bound solutions for face stability of circular tunnels in undrained clays. Géotechnique, **68**(1): 76–85. doi:10.1680/jgeot.16.T.028.

Zhang, J., Huang, H.W., and Phoon, K.K. 2013. Application of the kriging-based response surface method to the system reliability of soil slopes. Journal of Geotechnical and Geoenvironmental Engineering, **139**(4): 651–655. doi:10.1061/(ASCE)GT.1943-5606.0000801.

Zhao, Y., and Lu, Z. 2006. Fourth-Moment standardization for structural reliability assessment. Journal of Structural Engineering, **133**(7): 916–924. doi:10.1061/(ASCE)0733-9445(2007)133:7(916).

Zhou, W., Hong, H.P., and Shang, J.Q. 1999. Probabilistic design method of prefabricated vertical drains for soil improvement. Journal of Geotechnical and Geoenvironmental Engineering, **125**(8): 659–664. doi:10.1061/(ASCE)1090-0241(1999)125:8(659).

Zhu, D., Griffiths, D.V., Huang, J., and Fenton, G.A. 2017. Probabilistic stability analyses of undrained slopes with linearly increasing mean strength. Géotechnique, **67**(8): 733–746. doi:10.1680/jgeot.16.P.223.